Theoretical study of carrier confinement in a-Si–SiC quantum wells

Z. Q. Li and W. Pötz
Department of Physics, University of Illinois at Chicago, Chicago, Illinois 60680
(Received 21 October 1992)

We present a systematic theoretical analysis of carrier confinement in amorphous semiconductor quantum wells. Our study is based on a fourfold-coordinated continuous random-network model for the amorphous state. A semiempirical tight-binding approach and the recursion method are used to calculate the average electronic density of states of clusters consisting of typically 57 600 atoms. For narrow wells we find that the average local density of states near the well center exhibits these features both at the valence- and conduction-band edge. Comparison with calculations for the bulk and corresponding crystalline quantum wells allows the interpretation that quantum confinement effects due to the presence of barrier materials are responsible for these features in the density of states. For quantum well width below about 20 Å the onset of a gap formation which separates strongly localized states from extended conduction-band states is observed.

I. INTRODUCTION

During the past three decades a new class of semiconductors has been bred by heteroepitaxial growth of semiconductor heterostructures.[1] The most investigated and probably most interesting new properties of these materials are known as electronic quantum confinement effects (EQCE's). They are achieved by intentionally built-in mesoscopic band-gap variations and the wave nature of the electron. The formation of sub- and minibands in *crystalline* semiconductor heterostructures is well documented in the literature and represents a direct consequence of the spatially extended eigenfunctions (Bloch functions) of crystalline materials. The situation is rather different for amorphous semiconductor heterostructures. Although amorphous semiconductors and insulators display a variety of rather interesting physical properties and have been demonstrated to be of high technological importance, particularly when used in conjunction with crystalline materials, they have not yet reached the popularity of their crystalline counterparts. This may partially be due to the inherent complexity of amorphous systems which makes them considerably more difficult to characterize and study systematically than crystalline materials, both experimentally and theoretically. In particular, it has remained unclear whether EQCE's exist at all in amorphous semiconductor heterostructures. Only a limited number of isolated experimental investigations indicates that a quasi-two-dimensional density of states (DOS) is formed in amorphous quantum-well systems.[2–8] Due to the spatially localized nature of the eigenstates of (bulk) amorphous materials,[9] it may indeed be expected that EQCE's are not as pronounced as in heterostructures built from crystalline materials. Moreover, EQCE's may be suppressed or difficult to verify experimentally due to a lack of the k-vector conservation rule, as well as the presence of undesired defects which are not directly part of the amorphous state. In addition, growth-specific variations in the samples make reproducibility and comparison of results for samples grown in different laboratories difficult.

Amorphous semiconductor heterostructures represent interesting physical systems for several reasons. First, they are systems in which a mesoscopic long-range order is superimposed onto the disorder of the amorphous state. Systematic variation of the well width imposes a perturbation on the well layers in similar fashion as, for example, a homogeneous external magnetic field of adjustable strength. Therefore a study of quantum wells can provide information about bulk properties of amorphous materials. Depending on the spatial extent of the bulk electron eigenstates, associated energy levels will shift as a consequence of the vicinity of barriers. Thus, if one accepts the existence of a mobility edge in amorphous semiconductors which has been envisioned to rather sharply separate localized from extended states, enhanced separation of these two types of states may be expected due to quantum confinement effects.

As mentioned above, there is indeed some experimental evidence for EQCE's in amorphous semiconductor heterostructures. Photoluminescence has been used to investigate electronic states of a-Si:H–a-SiN:H systems.[3,7,10–12] Miyazaki, Ihara, and Hirose have measured the electric current through a-Si:H–a-SiN:H double-barrier structures and concluded that slight peaks observed in the I-V curve were due to confinement-induced resonant tunneling.[5] Unfortunately these peaks seem to be extremely weak, and complementary experimental data on the same structures in support of their claims were not included in the paper. This may leave some doubt as to the correct interpretation of the experimental data. Nebel *et al.* reported on a combination of optical and transport measurements performed on a-Si:H–a-$Si_{1-x}C_x$:H superlattices and found an increase in the optical band gap as well as evidence for the existence of quantized levels.[8] Sensitive photothermal modulation (PTM) spectroscopy has been used to investigate multilayered structures of a-Si:H and a-SiC:H.[6] An analysis of the PTM spectra in terms of a particle-in-a-box model was given in support of the conclusion that the steplike features in the spectra for well thicknesses below 5 nm were indeed a signature of quantum confinement effects.

The same authors previously reported on in-plane transport measurements which displayed an anomalous increase in the carrier diffusion length.[13] This may also be taken as an indication of EQCE's and, possibly, of an increased separation of localized and extended electronic states near the band edges. It should be noted that, by far, not all attempts to see EQCE's in amorphous systems have been successful.

A theoretical investigation of EQCE's in amorphous heterostructures is an equally delicate matter. Theoretical studies of dimensional quantization and tunneling in amorphous semiconductor heterostructures have remained limited in number and have generally been based on dramatic approximations.[14–16] Nonperiodicity, as well as the multitude of defects and impurities which may be present in real amorphous materials, makes an analysis of their electronic properties, based on microscopically realistic models, practically impossible. There are, however, a variety of tractable models for the atomic structure of amorphous semiconductors, in particular *a*-Si, which can correctly produce general structural features of the amorphous state, as well as general electronic properties in agreement with experiment when linked to a suitable formalism for the electronic structure.[17–19] One of the first truly successful computer-generated models for *a*-Si was developed by Wooten, Winer, and Weaire.[20] It is based on a continuous random network cluster of 216 atoms which is constructed from crystalline Si by elementary bond-switching operations and subsequent annealing procedures based on Keating-type potentials. With the advent of more powerful computers, molecular-dynamics simulations have also been used to generate structure models for the amorphous state, usually using Stillinger-Weber-type potentials.[21] In some instances, modified versions of the Stillinger-Weber potential have been used.[22,23] Simulations of amorphous semiconductor compounds have remained limited in number due to obvious additional complications.[24]

Here we report on a theoretical study of EQCE's in *a*-Si–SiC quantum wells. Due to the complexity of the problem posed here we adopt the simplest and perhaps most efficient approach which can be expected to provide the main physical features of confinement-induced changes which occur in the electronic density of states. We consider a hydrogen-free continuous random network model for *a*-Si of the kind proposed by Wooten, Winer, and Weaire.[20] Such a layer of "*a*-Si" is embedded between two cladding layers of crystalline SiC. EQCE's are identified by comparison of the density of states of this system with that of the *a*-Si layer enclosed between *c*-Si cladding layers. The local density of states (LDOS) is calculated using an efficient tight-binding-recursion-method scheme which we have previously applied to ternary semiconductor alloys.[25]

The present model for the atomic structure of the amorphous quantum well and a brief review of our electronic structure calculations are given in Sec. II. A systematic study of the electronic density of states as a function of well width, together with a discussion of our results and numerical details, is presented in Sec. III. Summary and conclusions are given in Sec. IV.

II. MODEL

For our theoretical study of EQCE's in amorphous semiconductors, we selected *a*-Si–SiC single quantum wells. Next to SiO_2 *a*-Si is certainly the most-studied example of an amorphous semiconductor. Except for strong lattice mismatch due to the short C-Si bond length of 1.88 Å versus 2.35 Å for the Si-Si bond in *c*-Si, $Si_{1-x}C_x$ provides an ideal barrier material for both top valence band states and the lowest conduction-band states of *a*-Si due to a favorable band offset.[26–28]

We have constructed a series of clusters, each consisting of 57 600 atoms, to represent *a*-Si–SiC quantum wells with layer thickness ranging from about 10 to 18 Å. Crystalline SiC layers have been used to keep the computational efforts as low as possible. Using such barriers, rather than *a*-SiC barriers, is certainly crude and, in particular, leads to somewhat artificial interfaces. However, we are interested merely in modifications in the LDOS within the *a*-Si layer. For this purpose, *c*-SiC fulfills at least the primary task of providing confining barriers for Si band-edge states and it is unlikely that the detailed nature of the electronic structure of the barriers is of importance for the local electronic density of states near the center of the *a*-Si well.

Our computational procedure is as follows. Originally a cubic cluster of crystalline Si is constructed by joining layers of Si in the [0,0,1] direction. Each layer contains 800 atoms. We use 72 layers. The dimensions of the cluster are approximately 100 Å×80 Å×80 Å, roughly corresponding to $72\times800=57\,600$ atoms. Periodic boundary conditions are used at the cluster surfaces throughout this work. Large clusters seem to be unavoidable for the present study. For one, we need to represent a well of certain thickness and the two neighboring barriers simultaneously. Second, rather than overall features we want to investigate details at the valence- and conduction-band edge and, thus, need a representative number of data points in the numerical DOS. Large cluster sizes have been made possible by the efficiency and relative simplicity of the present model, the numerical efficiency of our code, and the use of supercomputing facilities. In this original cluster of *c*-Si, a well region with [0,0,1] interfaces is identified at the center of the cluster. This slab of Si is converted into a continuous random network model of *a*-Si, largely following a procedure suggested by Wooten *et al.*[20,29] For this purpose, a large number of elementary bond switches is performed in the well region to destroy structural features associated with *c*-Si. These switching processes are followed by a lattice relaxation guided by a Keating potential which, in turn, is followed by several stages of annealing cycles to bring bond-length and bond-angle fluctuations into close agreement with experimental data for *a*-Si. Using the notation of Ref. 30, the Keating parameters for *a*-Si $\alpha=48.5$ (N/m) and $\beta=13.8$ (N/m) were chosen.

The position of Si atoms in the barrier regions which, up to now, has been held fixed, is now relaxed to reduce strain at the interfaces. We find that the propagation of lattice distortion into the *c*-Si layers is limited to about two layers of *c*-Si per cladding layer. Finally, every other

Si atom within the designated barrier regions is replaced by C.

This procedure leads to a somewhat artificial description of the heterointerfaces due to the neglect of the lattice mismatch between a-Si and SiC. However, using a *continuous random network* for the interface region which accounts for lattice mismatch seems to be even more artificial. In reality, it must be expected that the lattice mismatch is primarily accommodated by interfacial defects, such as dangling bonds and impurities, rather than elastic strain. In crystalline materials lattice mismatch may be accommodated by both (uniform) elastic strain and interfacial defects. The latter frequently lead to dislocations which should not be of importance in amorphous systems. In hydrogenated material, however, one may expect a high concentration of H at the interface, partially eliminating dangling bonds. This has indeed been observed experimentally.[31] Thus there will be little additional lattice distortion in neither a-Si nor SiC owing to lattice mismatch and, except for H incorporation, our model should be reasonably close to reality. Effects on the LDOS due to H incorporation have been investigated both experimentally and theoretically.[32–34] Primarily, H incorporation is believed to influence the optical band gap by reducing the strength of the $pp\pi$ bond, leading to a downward shift of the upper valence-band edge. For H-free a-Si, an optical band gap of 1.5 eV has been measured.[35] Increase of the H concentration monotonically raises the optical band gap. Typical band gaps of a-Si:H samples lie around 1.8 eV. Several forms of H incorporation may be envisioned.[36]

The electronic structure of our cluster was obtained by following a procedure used previously to investigate ternary alloys.[25] Using a nearest-neighbor sp^3s^* tight-binding (TB) model, a Hamiltonian matrix is associated with the cluster. For the a-Si layer we use c-Si matrix elements which are rescaled according to the local environment of a specific Si atom.[37,25] Within the barrier, we use SiC TB parameters based on the SiC lattice constant. The diagonal TB elements of SiC were shifted so that experimental values for the band offsets are achieved. Here, we used 0.53 eV for the conduction band and 0.7 eV for the valence band. TB parameters used here are listed in Table I. The resulting TB Hamiltonian matrix was used to evaluate the LDOS for sites within the well by means of the recursion method.

Calculation of the LDOS requires evaluation of diagonal elements of the Green's function for given state μ and lattice site l, $|l\mu\rangle$, which may be written in the form

$$\langle l\mu|G(Z)|l\mu\rangle = \cfrac{1}{Z-a_0-\cfrac{b_1^2}{Z-a_1-\cfrac{b_2^2}{Z-a_2-\cfrac{b_3^2}{\ddots}}}} . \tag{1}$$

$\{a_n\}$ and $\{b_n\}$, respectively, are the diagonal and off-diagonal matrix elements of the linear-chain Hamiltonian which is obtained from the original matrix by a suitable sequence of unitary transformations. The LDOS is given by

$$n(E,l\mu) = -\frac{1}{\pi}\lim_{\delta\to 0+}\mathrm{Im}\langle l\mu|G(Z)|l\mu\rangle . \tag{2}$$

Here $Z=E+i\delta$ and δ is a small imaginary part which must be chosen suitably. Our value $\delta=0.024$ is based on a detailed investigation of crystalline quantum wells of the same cluster size. A suitable choice of δ is essential. If δ is chosen too small spurious oscillations may occur in the LDOS. On the other hand, if δ is too large essential features in the LDOS may be overlooked. Here, the LDOS per atomic site is calculated as an average over s, s^*, and p orbitals.

III. RESULTS

Prior to application to amorphous quantum wells, we tested our computer model by constructing clusters of 512 atoms to model bulk a-Si. Elementary bond switches, in which pairs of nearly parallel bonds are cut and reconnected, were used to produce an unrelaxed fourfold coordinated continuous random network.[20] For the present cluster size, we found that an initial switching rate of about 1.6 is required per atom to sufficiently destroy crystalline features of the network. This leads to a 20° average angle fluctuation $\Delta\theta$ and 7.5% relative bond-length fluctuation in the network. Subsequent gradual annealing, using typically 30 000 trial switches and gradual lowering of the temperature from $kT=0.45$ to 0.2 eV, leads to both bond-angle and bond-length fluctuations close to experimental findings. Plots of the overall DOS for two different cases can be found in Figs. 1 and 2. It can be seen, by comparison with c-Si (dotted line), that the sample with $\Delta\theta=10.6°$ exhibits somewhat more crystalline features than the sample with $\Delta\theta=12.4°$. The en-

TABLE I. Matrix elements of the tight-binding Hamiltonian in eV and bond length d in Å. a denotes anion and c cation.

	E_{sa}	E_{sc}	E_{pa}	E_{pc}	E_{s^*a}	E_{s^*c}	d
Si	−4.200	−4.200	1.715	1.715	6.685	6.685	2.35
SiC	−8.404	−4.796	2.123	4.347	9.653	9.317	1.88
	V_{ss}	$V_{sp\sigma}$	$V_{ps\sigma}$	$V_{pp\pi}$	$V_{pp\sigma}$	$V_{s^*p\sigma}$	$V_{ps^*\sigma}$
Si	−2.075	2.481	2.481	−0.715	2.716	2.327	2.327
SiC	−3.118	4.130	4.000	−0.706	3.689	3.755	1.874

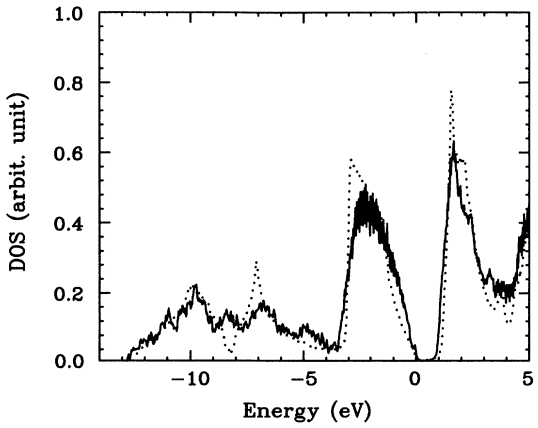

FIG. 1. The DOS of a-Si within a 512-atom network cluster with bond-angle fluctuation $\Delta\theta = 10.6°$ and relative-bond-length variation $\Delta R/R = 2.97\%$.

ergy bands are significantly smeared out and are, generally, in good agreement with experiment,[38] as well as with earlier studies using smaller clusters and predictions from general considerations based on TB models.[39–41] We intentionally kept $\Delta\theta$ slightly above experiment to be sure not to underestimate disorder. A convolution of valence and conduction-band DOS of the structure with $\Delta\theta = 10.6°$ was used to estimate the absorption coefficient. It was found that the Tauc plot closely resembles that of a realistic sample, however, the optical bandgap of 1.3 eV lies clearly below experimental data on a-Si:H with a value of typically 1.7 eV.[42] The latter is largely due to lack of hydrogen in our model system.

We used this network model of a-Si to calculate the average LDOS near the upper-most valence-band edge and the lowest conduction-band edge for several quantum well structures, as well as bulk systems. In the present paper, we discuss quantum wells with seven, nine, and thirteen atomic layers of a-Si. This corresponds to layer thicknesses between about 10 and 18 Å. Table II lists the number of layers, the final standard deviation in the Si-Si bond-angle, average relative bond-length fluctuation, and the final bond switch rate per atom which characterize the different a-Si well layers. The TB parameters for c-Si on which our calculations are based were taken from a fit to experimental data.[43] For c-SiC, the TB parameters were obtained by fit to experiment and nonlocal empirical pseudopotential calculations.[44–46] The TB parameters may be found in Table I. The energy dispersion which was achieved for c-Si and c-SiC is given in Figs. 3 and 4, respectively. Although there are some deficiencies in this nearest-neighbor model regarding the (upper) conduction bands, it rather accurately reproduces experimental data in the vicinity of the main energy gap, which is of primary interest here.

TABLE II. Characteristic data for the SiC–a-Si–SiC quantum wells. All parameters pertain to the a-Si region.

Sample	Layers	$\Delta\theta$ (deg)	$\frac{\Delta R}{R}$ (%)	Switch rate
1	7	10.27	2.78	1.47
2	9	9.280	2.37	1.43
3	13	10.84	2.37	1.43

The average LDOS at *well center* was obtained by averaging over at last 40 randomly picked sites which are located within a 2-Å-thick layer at the center of the well. To aid interpretation of our data for a-Si/SiC quantum wells, we also looked at model structures in which cladding layers of pure c-Si were used. Due to the absence of any significant band offsets at the interfaces of such structures, they were used as reference systems to which the amorphous quantum wells were compared. Furthermore, we performed calculations for corresponding crystalline quantum wells, again neglecting lattice mismatch at the heterointerfaces. This model system was investigated to obtain an understanding of how clearly the formation of a quasi-two-dimensional density of states is reflected in the LDOS of *crystalline* materials, where the formation of

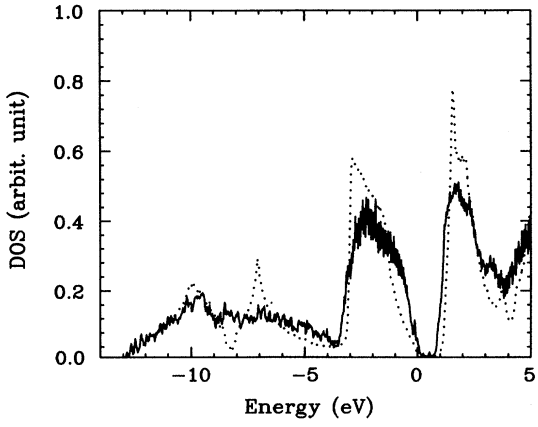

FIG. 2. The DOS of a-Si within a 512-atom network cluster with bond-angle fluctuation $\Delta\theta = 12.4°$ and relative-bond-length variation $\Delta R/R = 3.37\%$.

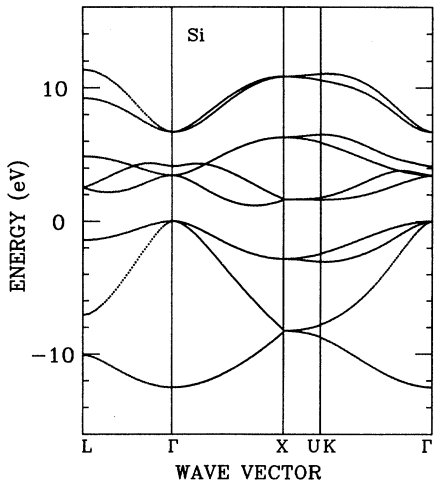

FIG. 3. The band structure of c-Si as obtained from the sp^3s^* model.

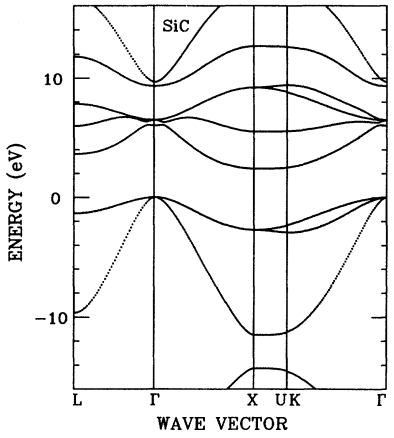

FIG. 4. The band structure of *c*-SiC as obtained from the sp^3s^* model.

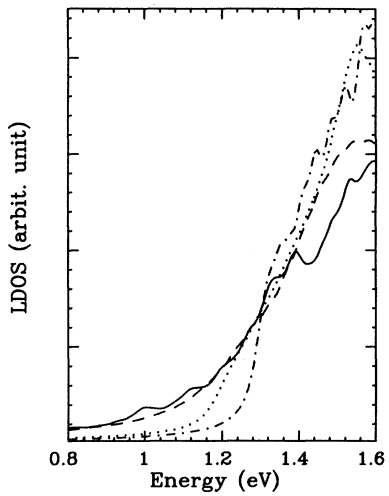

FIG. 6. Average LDOS at the center of the nine-layer Si-SiC well near the bottom of the conduction band. Solid line, *a*-Si–SiC; dashed line, *c*-Si–*a*-Si; dot-dashed line, *c*-Si–SiC; dotted line, *c*-Si.

electronic subbands has been well established and is quantitatively well understood. Furthermore, this allows selection of a suitable value for δ, as well a direct comparison with effects observed in the LDOS of the amorphous counterpart. Results for the site-averaged LDOS for all structures are summarized in Figs. 5–10, whereby solid, dashed, dot-dashed, and dotted lines refer to *a*-Si–SiC quantum wells, *a*-Si–Si structures, *c*-Si–SiC quantum wells, and bulk *c*-Si, respectively. The energy scale is such that zero coincides with the band edge of *c*-Si.

Our narrowest well consists of seven layers of Si, which corresponds to a well width of about 10 Å. Results for the conduction-band edge are given in Fig. 5. The LDOS of the amorphous quantum well (solid line) clearly displays several features: in the band tail up to about 1.1 eV virtually no change occurs in the LDOS. Then the LDOS suffers a clearly visible drop which is followed by a rather sharp increase, when compared to the *a*-Si–Si structure (dashed line). This drop occurs roughly at the energy where bulk *c*-Si (dotted line) has its conduction-band edge. Several steplike features can be clearly resolved above about 1.3 eV. This energy corresponds to the region where the LDOS of bulk *c*-Si and the crystalline quantum well (dot-dashed line) cross. Although located at roughly the same energy, the formation of the lowest confinement level is, for this well thickness, much more pronounced for the crystalline quantum well, while higher levels produce signatures of similar strength. It should be kept in mind that the LDOS takes into account the magnitude of the wave function at the particular atomic site, as well as that the conduction-band edge of *c*-Si is characterized by two different effective electron masses.

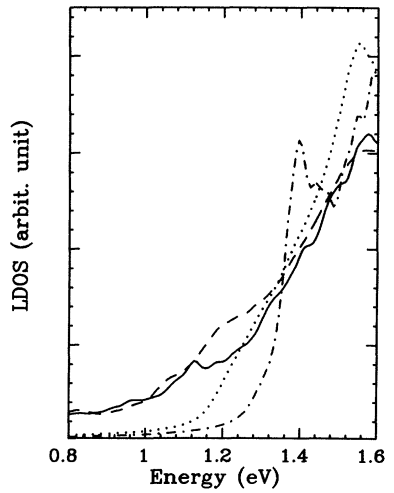

FIG. 5. Average LDOS at the center of the seven-layer Si-SiC well near the bottom of the conduction band. Solid line, *a*-Si–SiC; dashed line, *c*-Si–*a*-Si; dot-dashed line, *c*-Si–SiC; dotted line, *c*-Si.

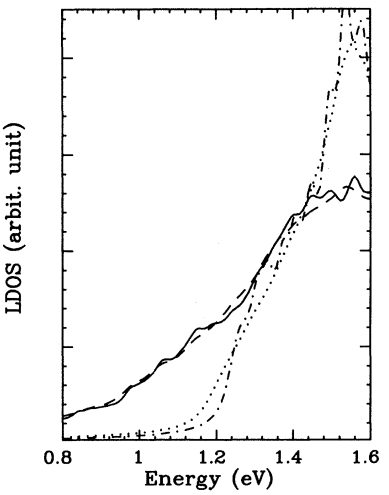

FIG. 7. Average LDOS at the center of the thirteen-layer Si-SiC well near the bottom of the conduction band. Solid line, *a*-Si–SiC; dashed line, *c*-Si–*a*-Si; dot-dashed line, *c*-Si–SiC; dotted line, *c*-Si.

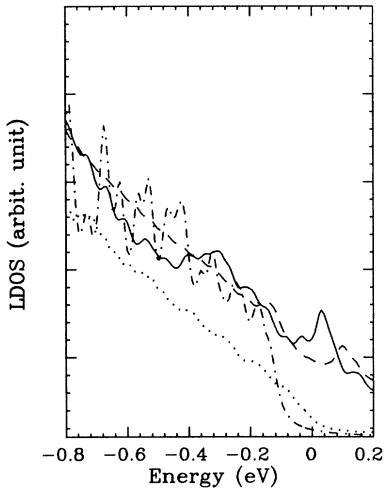

FIG. 8. Average LDOS at the center of the seven-layer Si-SiC well near the top of the valence band. Solid line, *a*-Si–SiC; dashed line, *c*-Si–*a*-Si; dot-dashed line, *c*-Si–SiC; dotted line, *c*-Si.

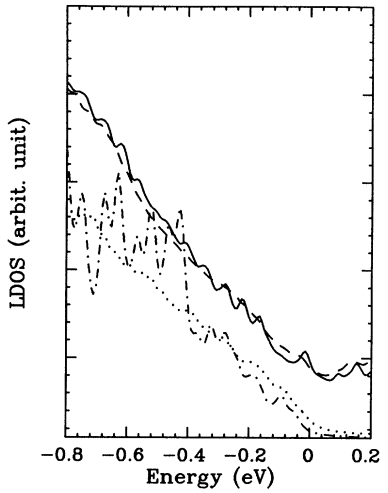

FIG. 10. Average LDOS at the center of the thirteen-layer Si-SiC well near the top of the valence band. Solid line, *a*-Si–SiC; dashed line, *c*-Si–*a*-Si; dot-dashed line, *c*-Si–SiC; dotted line, *c*-Si.

Considering a well which consists of nine layers of Si, a similar picture emerges in Fig. 6. Below the band edge of *c*-Si, i.e., in the "band-tail" regime of *a*-Si, the average LDOS suffers merely small changes, indicating a localization length of states in this energy regime comparable to or below well width. The regime of a depressed LDOS which was observed for the seven-layer well now is less pronounced. However, as before, the LDOS clearly displays the signature of confinement effects above the energy where the bulk *c*-Si DOS (dotted line) crosses the *c*-Si–SiC LDOS (dot-dashed line). Electronic confinement is also evident for the *c*-Si–SiC well. This scenario repeats itself for our widest well consisting of thirteen Si layers, corresponding to about 18 Å. Changes in the density of tail states are further reduced due to the increased well width. Near the energy corresponding to the band edge of *c*-Si, a small dip in the LDOS of the *a*-Si–SiC well is evident and followed by a rapid, steplike increase in the density of states. The latter is again the signature of quantum confinement effects on extended *a*-Si states. It should be mentioned that, even when 40 sites are considered, details in the shape of the average LDOS depend somewhat on the sites over which the average is performed. However, the qualitative features mentioned above and, most importantly, the position of the steps above the *c*-Si band edge is maintained.

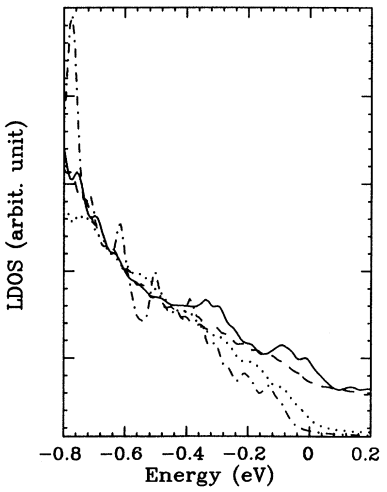

FIG. 9. Average LDOS at the center of the nine-layer Si-SiC well near the top of the valence band. Solid line, *a*-Si–SiC; dashed line, *c*-Si–*a*-Si; dot-dashed line, *c*-Si–SiC; dotted line, *c*-Si.

We interpret these findings as a confirmation of the picture envisioned in the Introduction. The band-tail states have a high degree of localization and remain virtually unaffected by the presence of barriers, unless located at the interface. However, with decreasing well width, states centered relatively close to an interface and/or with relatively large spatial extent, the latter corresponding to an energy eigenvalue close to, or above, the *c*-Si band edge, get pushed up in energy, thus opening a "gap" between localized and extended states. For narrow wells, such as considered here, clear quasi-two-dimensional signature is evident in the LDOS. As one would expect, this structure is generally weaker than for the crystalline counterpart.

We also performed an analysis of confinement effects at the upper valence-band edge. Figures 8–10 give a comparison of the average LDOS (at well center) for *a*-Si–SiC (solid line), *a*-Si–Si (dashed line), *c*-Si–SiC (dot-dashed line), and *c*-Si (dotted line). In spite of the relatively large valence-band offset of 0.7 eV, large hole masses cause that quantum confinement effects are somewhat more difficult to resolve in the LDOS at the valence-band edge. This also holds for the present *crystalline* materials. Nevertheless, barrier-induced modifications are clearly resolved. In the crystalline case, a lowering of the band edge and the formation of a subband structure is ob-

served, with the lowest subband position moving from about 0.10 to 0.03 eV as the well width is increased from seven to thirteen atomic monolayers. For a-Si–SiC, where disorder leads to a considerable increase in the LDOS close to the band edge (dashed versus dotted line), the situation is less obvious. Even below the bulk valence-band edge, barriers seem to provide variations in the average LDOS. As the barrier height is increased, band-tail states near 0 eV are shifted to lower energies when the well width becomes extremely small. These features in the structure may be due to states located at the interface where our model provides somewhat larger bond-angle fluctuations than in a-Si. This is indicated by the fact that these peaks are also present in the a-Si–c-Si structures, that bond-angle fluctuations primarily affect the valence band edge, and that these states are remarkably sensitive to the presence of barriers. At somewhat lower energies, additional structure arises which, by comparison with the crystalline case, may be interpreted as being due to the formation of a confinement-induced sub-band-like energy structure. In order to verify that $\delta=0.024$ was not too small a choice and did not lead to spurious fluctuations, we also evaluated the LDOS for $\delta=0.04$. For this value, part of the subband structure of the crystalline quantum wells is smeared out. In particular, the lowest confinement levels which occur in the *crystalline* quantum wells are lost, indicating that $\delta=0.04$ is too large a choice. The main features, both for crystalline and amorphous structures, are the same as in Figs. 8–10.

Several other investigations have been performed. First we compared the LDOS for neighboring sites (bonded and nonbonded) at well center. Strictly equivalent atomic sites cannot be identified in amorphous structures. Thus strongly site-dependent variations in the LDOS may be expected. As a representative example we compare the LDOS of the nine-layer well for two neighboring nonbonded sites at well center in Figs. 11 and 12. Solid lines pertain to the quantum-well case, whereas dashed lines pertain to the corresponding a-Si–c-Si structure. Strong effects due to the presence of confining barriers can clearly be resolved. Moreover, a strong site dependence in the LDOS is found, both with and without confining barriers. This site dependence must be attributed to variations in the local environment around a specific site. Remarkably, however, common changes in the LDOS survive site averages within a given well layer which is parallel to the hetero-interfaces, as documented in Figs. 5–10.

We also tested our interpretation of the steplike density of states as being due to electronic quantum confinement effects by inspection of the average LDOS as a function of distance from the interface. In Fig. 13, the average LDOS is plotted for the nine-layer a-Si–SiC quantum well at well center (solid line), two layers (2.71 Å) to the "right" of the center (dashed line) and two layers to the "left" of the center (dotted line). It can be seen that the steps above the c-Si band edge which we identified as due to the lowest confinement-induced levels are still observable two layers away from well center. The lowest peak which is clearly resolved in all three curves lies at about 1.24 eV. Peaks below 1.2 eV are not common to all three curves and thus may be traced back to localized states which happen to lie close to one of the interfaces.

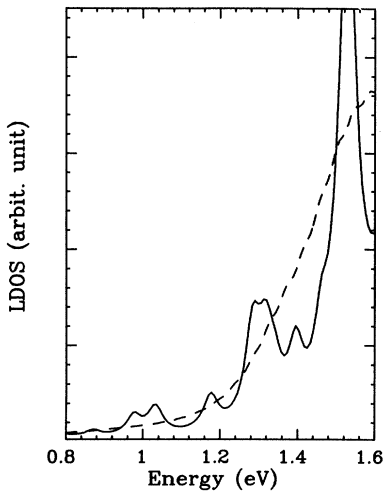

FIG. 11. LDOS for a site at the nine-layer a-Si–SiC well center near the edge of the conduction band. Solid line, a-Si–SiC; dashed line, a-Si–c-Si.

IV. SUMMARY AND CONCLUSIONS

We have performed a model study of electronic quantum confinement effects (EQCE's) in amorphous Si-SiC quantum-well structures. Present calculations are based on a continuous random network for a-Si, which is obtained by elementary bond switches and subsequent simulated annealing, closely following a previously developed procedure.[20] Large clusters with up to 57 600 atoms and periodic boundary conditions were constructed to model amorphous and crystalline Si and Si-SiC quantum wells. The LDOS of these structures was evaluated within a TB

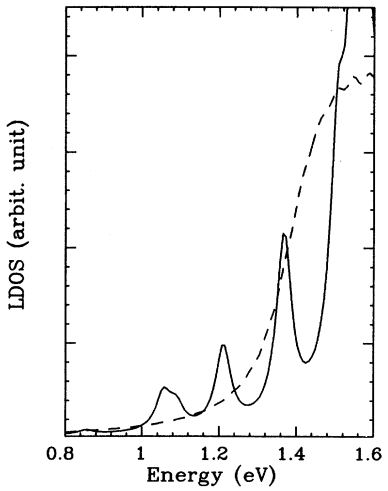

FIG. 12. LDOS for a site at the well center neighboring but nonbonded to the site chosen in the Fig. 11. Solid line, a-Si–SiC; dashed line, a-Si–c-Si.

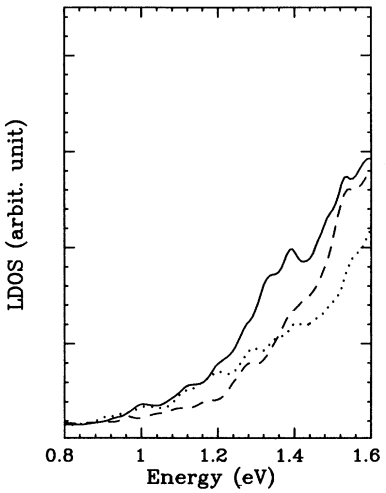

FIG. 13. Average LDOS for a nine-layer a-Si–SiC well. Solid line, at the well center; dashed line, two layers (2.71 Å) to the "right" of the center; dotted line, two layers to the "left" of the center.

model for covalent semiconductors by means of the recursion method.

Comparison of the average density of states at well center between a-Si–SiC and a-Si–c-Si model structures clearly exhibits electronic quantum confinement effects due to the presence of high barrier layers in a-Si–SiC structures. In our calculations, well thicknesses were varied from about 10 to about 18 Å. This interpretation of the LDOS was aided by comparative studies of equivalent c-Si quantum wells, as well as a study of the profile of the LDOS perpendicular to the heterointerfaces. For these extremely narrow wells, we also observe the onset of the formation of an energy gap near the conduction band edge at energies below the two-dimensional peaks. We interpret this effect as a consequence of a general energy dependence of the spatial extent of the electronic eigenfunctions of the amorphous system. In the band tails, the eigenfunctions are predominantly confined to within a few angstroms, whereas deeper into the band, the eigenfunctions adopt a more crystalline Bloch functionlike character. Thus confinement effects tend to separate localized and extended electronic states. This picture is in agreement with the temperature dependence of the carrier mobility in amorphous semiconductors, such as a-Si, and the notion of a mobility edge which separates localized from extended states. In our model, the mobility edge in the conduction band occurs in an energy region which lies slightly above the conduction band edge of the crystalline bulk material. As the c-Si band gap lies below the experimental optical band gap for a-Si it is unlikely that the onset to a formation of a gap can be verified by optical measurement. However, enhanced in-plane mobility has been reported in thin a-Si–SiC multiple quantum wells.[13] Such an effect might be attributed to an enhanced separation of localized and extended states due to confinement.

Similar to crystalline quantum wells, the signature of quantum confinement effects is somewhat less pronounced at the valence-band edge, however, it is still clearly resolvable for narrow quantum wells.

Although quantitatively successful for isovalent ternary alloys, the present model, when applied to a-Si–SiC quantum wells, must be considered a compromise between a realistic representation of amorphous quantum-well structures and simplicity which makes such an analysis feasible. Due to the adoption of a strictly fourfold-coordinated continuous random network, it does not account for structural defects such as vacancies, voids, and dangling bonds. Any of these defects may be expected to reduce EQCE's. Moreover, hydrogen, which is generally present in real systems, has not been incorporated into our model up to now. This is possible, in principle, following a bond-cut-and-switch procedure which is similar to the one used here to produce the continuous random network. This and other incorporation mechanisms were left out simply to restrict the computational effort. However, the encouraging first results from this study make more realistic models for a-Si:H–a-SiC:H heterostructures desirable. The presence of H is well known to increase the (optical) band gap. Thus a more direct comparison with experiment would be possible. Moreover, hybrid models with molecular dynamics approaches[19,47] may be useful for a more detailed understanding of the formation of amorphous heterointerfaces.

ACKNOWLEDGMENTS

This project was supported in part by the U.S. Army Research Office. Computer time was provided by the NSF through the National Center for Supercomputing Applications and the National Center for Computational Electronics, University of Illinois at Urbana-Champaign. One of us (W.P.) would also like to acknowledge the hospitality he received at the Walter Schottky Institute, Technical University Munich, and the Department of Theoretical Physics, University of Graz. Helpful discussion of experimental data with Dr. R. Schwarz is acknowledged.

[1]See review articles, for example, V. Narayanamurti, Phys. Today **37** (10), 24 (1984); M. J. Kelly and R. J. Nicholas, Rep. Prog. Phys. **48**, 1699 (1985); L. L. Chang, in *Layered Structures and Epitaxy*, edited by J. M. Gibson, B. C. Osburn, and R. M. Tromp, MRS Symposia Proceedings No. 56 (Materials Research Society, Pittsburgh, 1986), p. 267.

[2]H. Munekata and H. Kukimoto, Jpn. J. Appl. Phys. **12**, 213 (1982).

[3]B. Abeles and T. Tiedje, Phys. Rev. Lett. **51**, 2003 (1983).

[4]C. R. Wronski, P. D. Persans, and B. Abeles, Appl. Phys. Lett. **49**, 569 (1986).

[5]Seiichi Miyazaki, Yohji Ihara, and Masatake Hirose, Phys. Rev. Lett. **59**, 125 (1987).

[6]K. Hattori, T. Mori, H. Okamoto, and Y. Hamakawa, Phys.

Rev. Lett. **60**, 825 (1988).
[7]W. C. Wang and H. Fritzsche, J. Non-Cryst. Solids **97 & 98**, 919 (1987); in *Amorphous Silicon and Related Materials,* edited by Hellmut Fritzsche (World Scientific, Singapore, 1989), Vol. B, p. 779.
[8]C. E. Nebel, F. Kessler, G. Bilger, G. H. Bauer, Y. L. Jiang, H. L. Hwang, K. C. Hsu, and C. S. Hong, in *Amorphous Silicon Technology,* edited by Aran Madan, M. J. Thompson, P. C. Taylor, P. G. LeComber, and Y. Hamakawa, MRS Symposia Proceedings No. 118 (Materials Research Society, Pittsburgh, 1988), p. 361.
[9]Richard Zallen, *The Physics of Amorphous Solids* (Wiley-Interscience, New York, 1983).
[10]S. Kalem, Phys. Rev. B **37**, 8837 (1988); Superlatt. Microstruct. **3**, 325 (1988).
[11]Masataka Hirose, Seiichi Miyazaki, and Naoki Murayama, in *Tetrahetrally-Bonded-Amorphous Semiconductors,* edited by D. Alder and H. Fritzsche (Plenum, New York, 1985), p. 441.
[12]Chun Gen, V. Yu. Kaznacheev, and A. É. Yunovich, Fiz. Tekh. Poluprovodn. **25**, 1681 (1992) [Sov. Phys. Semicond. **25**, 1011 (1991)].
[13]K. Hattori, T. Mori, H. Okamoto, and Y. Hamakawa, Appl. Phys. Lett. **51**, 1297 (1987).
[14]W. Pötz and Z. Q. Li, Solid State Electron. **32**, 1353 (1989).
[15]M. E. Raikh, S. D. Baranovskii, and B. I. Shklovskii, Phys. Rev. B **41**, 7701 (1990).
[16]N. Porras-Montenegro, and E. V. Anda, Phys. Rev. B **43**, 6706 (1991).
[17]See the review article G. Etherington, A. C. Wright, J. T. Wenzel, J. C. Dore, J. H. Clarke, and R. N. Sinclair, J. Non-Cryst. Solids **48**, 265 (1982).
[18]W. Y. Ching, C. C. Lin, and Lester Guttman, Phys. Rev. B **16**, 5488 (1979); J. L. Mercer, and M. Y. Chou, *ibid.* **43**, 6768 (1991).
[19]J. M. Holender and G. J. Morgan, J. Phys. Condens. Matter **4**, 4473 (1992).
[20]F. Wooten, K. Winer, and D. Weaire, Phys. Rev. Lett. **54**, 1392 (1985).
[21]Frank H. Stillinger and Thomas A. Weber, Phys. Rev. B **31**, 5162 (1985).
[22]R. Biswas and D. R. Hamann, Phys. Rev. B **36**, 6434 (1987).
[23]J. M. Holender and G. J. Morgan, J. Phys. Condens. Matter **3**, 7241 (1991).
[24]See, for example, G. A. N. Connell and R. J. Temkin, Phys. Rev. B **12**, 5323 (1974); Iwao Ohdomari, Yukio Yamakoshi, Takehiko Kameyama, and Hiroyuki Akatsu, J. Non-Cryst. Solids **89**, 303 (1987).
[25]Z. Q. Li and W. Pötz, Phys. Rev. B **46**, 2109 (1992); **43**, 12 670 (1991).
[26]John Robertson, J. Non-Cryst. Solids **97&98**, 863 (1987).
[27]S. G. Meikle, Y. Hatanaka, Y. Suzuki, and G. Shimaoka, in *Amorphous and Crystalline Silicon Carbide,* edited by G. L. Harris and C. Y. -W. Yang (Springer-Verlag, Berlin, 1989), p. 161.
[28]M. Cuniot and N. Lequeux, Philos. Mag. B **64**, 723 (1991).
[29]F. Wooten and D. Weaire, J. Non-Cryst. Solids **114**, 681 (1989).
[30]P. N. Keating, Phys. Rev. **145**, 145 (1966).
[31]R. Schwarz, T. Fischer, P. Hanesch, T. Muschik, J. Kolodzey, H. Cerva, H. L. Meyerheim, and B. M. U. Scherzer, Appl. Surf. Sci. **50**, 456 (1991).
[32]E. N. Economou and D. A. Papaconstantopoulos, Phys. Rev. B **23**, 2042 (1981); D. A. Papaconstantopoulos and E. N. Economou, *ibid.* **24**, 7233 (1981).
[33]L. Ley, in *The Physics of Hydrogenated Amorphous Silicon II,* edited by J. D. Joannopoulos and G. Lucovsky (Springer-Verlag, Berlin, 1984), p. 61.
[34]G. D. Cody, J. Non-Cryst. Solids **141**, 3 (1992).
[35]H. Shirai, D. Das, J. Hanna, and I. Shimuzu, Appl. Phys. Lett. **59**, 1096 (1991).
[36]W. Y. Ching, D. J. Lam, and C. C. Lin, Phys. Rev. B **21**, 2378 (1980).
[37]J. C. Slater and G. F. Koster, Phys. Rev. **94**, 1409 (1954).
[38]L. Ley, S. Kowalczyk, R. Pollack, and D. A. Shirly, Phys. Rev. Lett. **29**, 1088 (1972).
[39]R. Biswas, C. Z. Wang, C. T. Chan, K. M. Ho, and C. M. Souklis, Phys. Rev. Lett. **63**, 1491 (1991).
[40]S. K. Bose, K. Winer, and O. K. Anderson, Phys. Rev. B **37**, 6262 (1988).
[41]F. Yonezawa and M. H. Cohen, in *Fundamental Physics of Amorphous Semiconductors,* edited by F. Yonezawa (Springer-Verlag, Berlin, 1981), p. 119.
[42]R. Schwarz (private communication).
[43]P. Vogl, P. Hjalmarson, and John D. Dow, J. Phys. Chem. Solids **44**, 365 (1983).
[44]L. A. Hemstreet and C. Y. Fong, Solid State Commun. **9**, 643 (1971); Phys. Rev. B **6**, 1464 (1972).
[45]S. Nishino, J. A. Powell, and H. A. Will, Appl. Phys. Lett. **42**, 460 (1983).
[46]W. L. Choyke and L. Patrick, Phys. Rev. **187**, 1041 (1969).
[47]Normand Mousseau and Laurent J. Lewis, Phys. Rev. B **43**, 9810 (1991).